Evolution of Electronic Structure of Doped Mott Insulators: Reconstruction of Poles and Zeros of Green's Function

Shiro Sakai, Yukitoshi Motome, and Masatoshi Imada

Department of Applied Physics, University of Tokyo, Hongo, Tokyo 113-8656, Japan

(Received 29 August 2008; published 4 February 2009)

We study the evolution of metals from Mott insulators in the carrier-doped 2D Hubbard model using a cluster extension of the dynamical mean-field theory. While the conventional metal is simply characterized by the Fermi surface (pole of the Green function G), interference of the *zero surfaces* of G with the pole surfaces becomes crucial in the doped Mott insulators. Mutually interfering pole and zero surfaces are dramatically transferred over the Mott gap, when lightly doped holes synergetically loosen the doublon-holon binding. The heart of the Mott physics such as the pseudogap, hole pockets, Fermi arcs, in-gap states, Lifshitz transitions, and non-Fermi liquids appears as natural consequences of this global interference in the frequency space.

DOI: 10.1103/PhysRevLett.102.056404 PACS numbers: 71.10.Hf, 71.30.+h, 74.72.−h

Electronic structures of doped Mott insulators have intensively been debated since the discovery of high-T_c cuprates. While overdoped metals behave like a conventional Fermi liquid, an outstanding issue is how such metals evolve into a Mott insulator. Experimental studies on doped cuprates revealed anomalous metallic behavior in proximity to the Mott insulator. Among them angle-resolved photoemission spectroscopy (ARPES) found arclike spectra around the nodal points of the momenta $\mathbf{k} = (\pm\frac{\pi}{2}, \pm\frac{\pi}{2})$, with a pseudogap in the antinodal region of the Brillouin zone [1]. Moreover the high-resolution ARPES [2] and quantum oscillations of resistivity observed under magnetic fields [3] proposed the existence of a small closed Fermi surface, called the pocket, in contrast to the large surface expected in the normal Fermi liquid. These imply the emergence of non-Fermi liquids under a radical evolution of electronic structure upon doping.

Diverse theoretical proposals were made for the Mott physics of the 2D Hubbard model: The pseudogap was reproduced in various theories [4,5]. The exact diagonalization (ED) studies [6] further found a spectral weight transfer with doping from the upper Hubbard band (UHB) to the top of the lower Hubbard band (LHB), which created in-gap states. The arclike spectra were reproduced in the cluster perturbation theory [7], the dynamical cluster approximation [8], the cellular dynamical mean-field theory (CDMFT) [5,9–12], and the composite operator method (COM) [13]. Hole-pocket Fermi surfaces around the nodal points were suggested in a phenomenology [14], the CDMFT [10], the COM [13], and a variational-cluster approach [15]. A topological change of the Fermi surface, i.e., Lifshitz transition [16], from electronlike to holelike surfaces due to a correlation effect was analyzed [13,17]. A Lifshitz transition to electron pockets was also found upon electron doping [18]. Despite these achievements, a coherent picture of the Mott physics has not emerged yet.

In general, poles of the single-particle Green function $G(\mathbf{k}, \omega)$ at the frequency $\omega = 0$ define the Fermi surface. While Re G changes its sign across a pole through $\pm\infty$, Re G may also change the sign across a *zero* defined by $G = 0$. In the Mott insulator, the self-energy $\Sigma(\mathbf{k}, \omega)$ inside the gap diverges on a specific surface in the $\mathbf{k} - \omega$ space, which defines a zero surface of G. Since the Fermi surface disappears in the Mott insulator while the zero surface appears instead, the evolution of the zeros makes crucial effects at low doping and is imperative in understanding the Mott physics [10,14,19].

In this Letter we study the 2D Hubbard model using the CDMFT + ED method [10,20], and clarify the doping evolution of poles and zeros of G in the $\mathbf{k} - \omega$ space. By figuring out reconstruction of interfering poles and zeros in a wide ω range, fragmentary features are integrated into a coherent understanding of the Mott physics. Hole doping induces a dramatic reduction of doublon-holon binding energy, which squashes a pile of pole and zero surfaces into a low-energy region, creating in-gap states. The pseudogap is described by a squashed zero surface which is a remnant of the Mott gap. The zero surface bends a pole surface crossing the Fermi level, leaving hole pockets around $(\pm\frac{\pi}{2}, \pm\frac{\pi}{2})$. Fermi arc emerges from this structure when the neighboring zeros interfere with the spectral weight of the outer part of the pocket. With further doping, the Fermi surfaces undergo at least two continuous Lifshitz transitions before reaching a normal Fermi liquid with an electronlike Fermi surface.

The Hubbard Hamiltonian on a square lattice reads

$$H = \sum_{\mathbf{k}\sigma} \epsilon(\mathbf{k}) c^{\dagger}_{\mathbf{k}\sigma} c_{\mathbf{k}\sigma} - \mu \sum_{i\sigma} n_{i\sigma} + U \sum_{i\sigma} n_{i\uparrow} n_{i\downarrow}, \qquad (1)$$

where $c_{\mathbf{k}\sigma}$ ($c^{\dagger}_{\mathbf{k}\sigma}$) destroys (creates) an electron of spin σ with momentum $\mathbf{k}$, and $n_{i\sigma}$ is a spin density operator at site i. U represents the on site Coulomb repulsion, μ the chemical potential, and $\epsilon(\mathbf{k}) = -2t(\cos k_x + \cos k_y) - 4t' \cos k_x \cos k_y$, where t (t') is the (next-) nearest-neighbor transfer integral.

In the CDMFT, the infinite lattice of the model (1) is self-consistently mapped onto an N_c-site cluster embedded in infinite bath sites, which define an $N_c \times N_c$ dynamical mean-field matrix $g_0(i\omega_n)$ for the cluster in terms of Matsubara frequency ω_n. We employ the Lanczos-ED method to solve the cluster problem at zero temperature, where g_0 is fitted with a finite number of bath parameters and a fictitious temperature $1/\beta$ is introduced. We adopt 2-by-2 cluster ($N_c = 4$) coupled with 8 bath sites and $\beta = 100/t$ unless otherwise mentioned. We obtain, self-consistently, an $N_c \times N_c$ self-energy matrix $\Sigma_c(i\omega_n)$, whose elements are defined on sites within the cluster. Then we interpolate cluster quantities in the momentum space, to obtain the original infinite-lattice ones. To study poles and zeros of G simultaneously, after careful examination, we employ the cumulant periodization [10], where the cluster cumulant $M_c \equiv (i\omega_n + \mu - \Sigma_c)^{-1}$ is interpolated with a Fourier transformation cut by a cluster size N_c, $M(\mathbf{k}, i\omega_n) = \frac{1}{N_c}\sum_{i,j=1}^{N_c}[M_c(i\omega_n)]_{ij}e^{i\mathbf{k}\cdot(\mathbf{x}_i-\mathbf{x}_j)}$. After M is obtained, G and Σ on the original lattice are calculated with $G = [M^{-1} - \epsilon(\mathbf{k})]^{-1}$ and $\Sigma = i\omega_n + \mu - M^{-1}$, respectively. The Lanczos-ED method allows us to calculate G at real frequencies directly through a continued-fraction expansion [21], where $i\omega_n$ is replaced by $\omega + i\eta$ with a small positive factor η. Although we should be careful on the limitation of the present size of the cluster, this combination of the methods is appropriate as the state of the art in exploiting zero and pole structures on equal footing [22].

We start from electronic structure of the Mott insulator at half filling ($\delta = 0$; δ is the hole doping rate from half filling) for $t' = 0$ and $U/t = 8$. While an insulating phase caused by some symmetry breaking may show a similar feature, to capture the essence of the Mott physics, we assume a paramagnetic solution. Figure 1(a) shows the structure of poles (green surfaces) and zeros (red surfaces) of G in the $\mathbf{k} - \omega$ space. Here ω is measured from the highest occupied state [23] to compare with the doped case below. The zero surface around $0 < \omega < 3t$ (the most distinct red surface) represents the Mott gap, which separates UHB and LHB displayed by entangled pole and zero surfaces. The zero surface at the Mott gap touches the pole surfaces of the UHB (LHB) around (0,0) [(π, π)] at $\omega \simeq 3t$ ($\omega \simeq 0$). The distinct pole surface in the UHB persists up to $\omega \sim 4t$, and another distinct one appears around $5t < \omega < 7t$. These pole surfaces provide large weights for the density of states (DOS) per spin [Fig. 1(c)]. In other area, poles are disrupted due to a large imaginary part of Σ, making incoherent contributions.

We next dope holes. Comparing the result at $\delta = 0.09$ in Fig. 1(b) with Fig. 1(a), we see that high-energy ($|\omega| \gtrsim 5t$) structure does not change appreciably while the lower-energy ($|\omega| \lesssim 5t$) structure does: The pole surface at the bottom of UHB $\sim 3t$ in Fig. 1(a) is transferred to the lowest-energy pole surface in the piles above $\omega \simeq 0.2t$, squashing the zero surface just below it, as in Fig. 1(b)

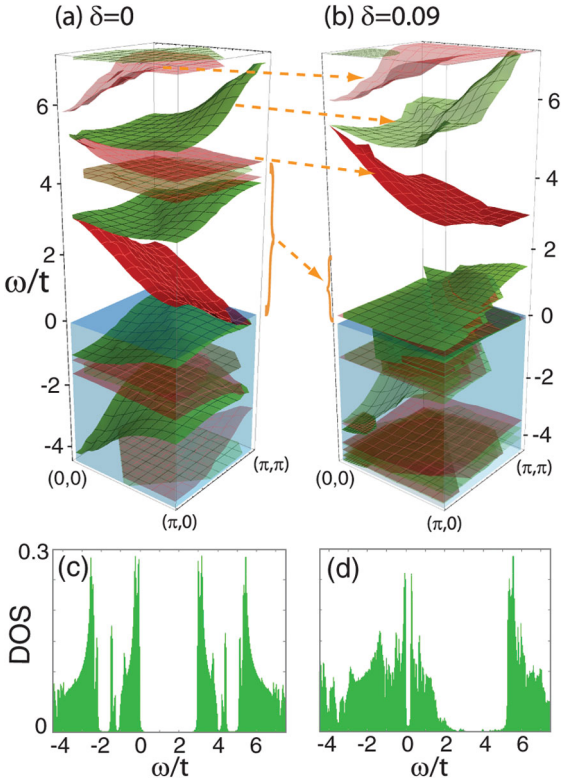

FIG. 1 (color). The $\mathbf{k} - \omega$ structure of poles (green) and zeros (red) of G for $t' = 0$, $U = 8t$ at (a) $\delta = 0$ and (b) 0.09. Occupied regions for an electron are filled with aqua. The transparency of pole (zero) surfaces reflects the imaginary part of the (inverse) self-energy (more transparent for larger imaginary part). (c) and (d) show DOS per spin at $\delta = 0$ and 0.09, respectively.

and also in Figs. 2(a) and 2(b). In addition, one of vague zero surfaces in the UHB piles in Fig. 1(a) turns to a distinct one at $\omega \sim 4t$ in Fig. 1(b). Correspondingly, the DOS at $\omega \simeq 3t$ in Fig. 1(c) is transferred to lower energies $\omega \lesssim 2t$ as shown in Fig. 1(d).

Let us focus on a low-energy structure. Figures 2(a) and 2(b) provide enlarged views of Fig. 1(b) near the Fermi level, in two different energy scales. A prominent feature is a small gap of width $\sim 0.2t$, described by a zero surface cutting the Fermi level. It is distinguished from the larger gap between the doped hole states and the UHB as shown in DOS in Fig. 1(d). A comparable pseudogap was found in earlier CDMFT studies [5,10].

As the zero surface around (π, π) extends to the region $\omega < 0$, near the zeros, the pole surface is pushed down below the Fermi level [Fig. 2(b)]. Meanwhile in the regions far away from zeros, the energy of poles increases with $|\mathbf{k}|$, reflecting the original dispersion $\epsilon(\mathbf{k})$. Hence, along the line from (0,0) to (π, π), for example, the pole energy initially increases, crossing the Fermi level, and then turns down around $(\frac{\pi}{2}, \frac{\pi}{2})$, crossing the Fermi level again. As a consequence, a hole pocket is formed around $(\frac{\pi}{2}, \frac{\pi}{2})$, accompanying a zero surface around (π, π), as found previously in Ref. [10] and also shown in Fig. 2(c).

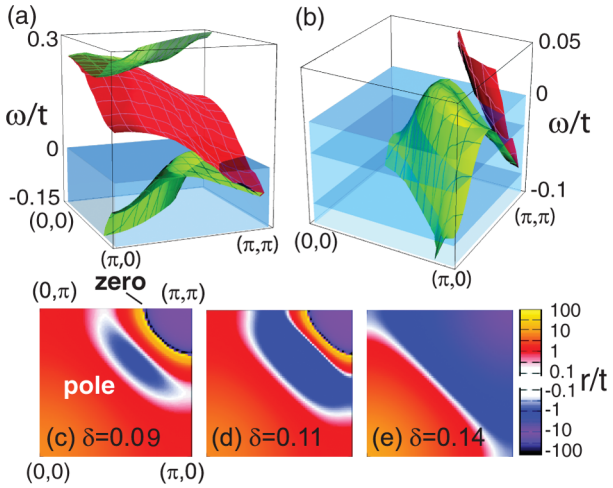

FIG. 2 (color). (a),(b) Close-ups of Fig. 1(b) at two different energy scales. Blue grade levels in (b) depict rigid-band shifts of the chemical potential. (c),(d),(e) $r(\mathbf{k}) \equiv \mathrm{Re}[G^{-1}(\mathbf{k}, 0)]$ in the first quadrant of the Brillouin zone for $t' = 0$ and $U = 8t$ at $\delta = 0.09$, 0.11 and 0.14, respectively. $r = 0$ ($\pm\infty$) defines the Fermi (zero) surface. We set $\eta = 10^{-4}t$ for these data.

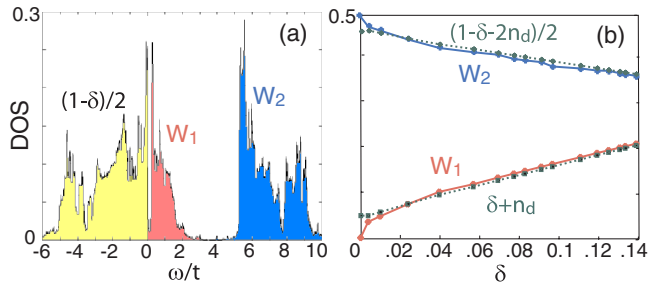

FIG. 3 (color online). (a) DOS at $\delta = 0.09$ [the same as Fig. 1(d)] and the definitions of weights W_1 and W_2. (b) δ dependence of W_1 and W_2 compared with the weights estimated from a simple analysis given by dashed lines (see the text). We set $\eta = 10^{-2}t$ for these data.

The metal-insulator transition occurs when the hole pockets shrink and vanish, indicating a topological nature of this transition [24]. Since the quick evolution for $\delta \lesssim 0.01$ elucidated below suggests a proximity to the first-order transition, the marginal quantum criticality [24] may have relevance.

To get further insight into the underlying physics of the dramatic restructuring, we study the doping evolution of DOS systematically. We calculate the weight integrated over energy ranges of $0 < \omega < 2.8t$ (in-gap weight), W_1, and that over $2.8t < \omega < \infty$ (UHB weight), W_2 [see Fig. 3(a)]. Figure 3(b) depicts δ dependences of W_1 and W_2, where W_1 (W_2) monotonically increases (decreases) with δ. The δ dependence of W_1 agrees well with $\delta + n_d$, where $n_d \equiv \langle n_{i\uparrow} n_{i\downarrow} \rangle$ is the doublon density. It is natural to have the weight proportional to δ in the rigid-band picture because it comes from the holes doped into the LHB, but there is an additional contribution n_d. This is interpreted as a strong-correlation effect as follows. The UHB corresponds to the process where an electron is added onto singly occupied sites, so that W_2 is roughly estimated to be $\frac{1}{2}(1 - \delta - 2n_d)$. Since the weight below the Fermi level is $\frac{1}{2}(1 - \delta)$, the remaining weight becomes $\delta + n_d$, which corresponds to W_1. This simple analysis neglecting dynamical fluctuations explains well the overall behavior of W_1 and W_2, as seen in Fig. 3(b).

A nontrivial finding, however, is that the weight n_d is quickly transferred from UHB to the top of LHB by tiny doping $\delta \lesssim 0.01$. Actually, the above simple analysis breaks down at tiny δ, where W_1 eventually and obviously vanishes as $\delta \to 0$. At $\delta = 0$ where this weight n_d is included in the UHB weight W_2, the same number of doublons and holons are tightly bound with the binding energy equal to the Mott gap $\sim 3t$. Hence one electron added to a hole site requires dissolution of the bound state and overcoming the Mott gap. The quick transfer of n_d from W_2 to W_1 means a quick reduction of the binding energy from $\sim 3t$ to $\sim 0.2t$ presumably due to an efficient screening of the doublon-holon interaction by the doped holes. Even with this screening, the binding energy though small still survives as the pseudogap. This quick reduction is promoted by a positive feedback, because the dissolved bound pairs further join in the screening. This constitutes a mechanism for the drastic restructuring in the Mott physics.

The next issue is how the hole-pocket Fermi surface accompanied by zeros of G in Fig. 2(c) evolves into a single electronlike Fermi surface expected in the normal Fermi liquid as δ increases further. Figures 2(c)–2(e) depict $r(\mathbf{k}) \equiv \mathrm{Re}[G^{-1}(\mathbf{k}, 0)]$ at $\delta = 0.09$, 0.11, and 0.14, respectively, showing how Fermi (zero) surfaces at $r = 0$ ($\pm\infty$) evolve. As δ increases from 0.09, the hole pocket continues to expand until it touches the Brillouin zone boundary ($|k_x|$ or $|k_y| = \pi$). Then it changes into two concentric Fermi surfaces around (π, π) through a Lifshitz transition, while the zero surface remains around (π, π) [Fig. 2(d)]. Further doping enlarges the unoccupied region (blue region) sandwiched by the two concentric Fermi surfaces. Then, the smaller Fermi surface around (π, π) merges with the zero surface and they are annihilated in pair, leaving a large holelike Fermi surface, which almost simultaneously transforms into a normal electronlike one through another Lifshitz transition [Fig. 2(e)]. For $\delta \gtrsim 0.14$ only a large electronlike Fermi surface is found. This evolution at the Fermi level is qualitatively understood from a rigid-band shift of the chemical potential in the structure of poles and zeros in Fig. 2(b), as drawn with blue grade levels. Detailed inspection of the two Lifshitz transitions shows continuities of the electron density as a function of μ and, hence, continuous transitions.

Apparently, the Luttinger sum rule [25] is violated for $\delta \lesssim 0.11$, while roughly satisfied for $\delta \gtrsim 0.14$. Since the

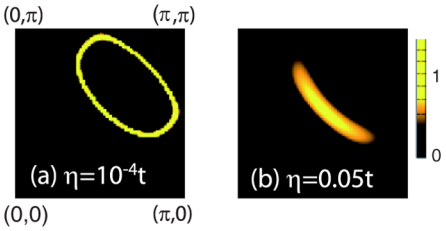

FIG. 4 (color online). $A(\mathbf{k}, 0) \equiv -\mathrm{Im}[G(\mathbf{k}, \omega + i\eta)]/\pi$ for $t' = -0.2t$, $U = 12t$, and $\delta = 0.09$ with (a) $\eta = 10^{-4}t$ and (b) $\eta = 0.05t$. Here we set $\beta = t/200$.

sum rule assumes an adiabatic continuity, it does not necessarily hold beyond the Lifshitz or zero-pole annihilation transitions at $\delta \sim 0.14$. Other calculations also pointed out the violation at small δ [10,17].

Next, we consider the effects of t'. Results for $\delta = 0.09$ (not shown) exhibit that $t' < 0$ elevates (lowers) the energy of poles around the nodal (antinodal) points, as expected from the original dispersion $\epsilon(\mathbf{k})$. The enhancement around the nodal points stabilizes the hole pocket while the reduction around antinodal points stabilizes a single holelike Fermi surface. Quantitative modifications caused by t' will be reported elsewhere.

Finally, we discuss how a Fermi arc emerges in the lightly doped region. Stanescu and Kotliar found that the zero surface reduces the spectral weight from the neighboring Fermi surface, resulting in a Fermi arc [10]. When we take the limit of $\eta \to 0^+$ in the Lanczos method, however, $\mathrm{Im}\Sigma$ becomes δ functions at zeros of G and has no contribution at the Fermi surface. In this limit, the spectral weight shows a closed pocket, not an arc, as demonstrated in Fig. 4(a) for a sufficiently small η. However, a larger η might be more realistic in describing experiments, where various extrinsic factors such as temperature, impurity, and phonon scatterings, and finite resolution of energy are inevitable [26]. A larger η broadens $\mathrm{Im}\Sigma$, which then suppresses the spectral weight close to the zeros as shown in Fig. 4(b). Thus the Fermi arc is reproduced by introducing a phenomenological broadening factor η in the present result. We note that Figs. 4(a) and 4(b) represent two different types of non-Fermi liquids.

To summarize, we have shown that key elements of the Mott physics such as in-gap states, hole pocket, Fermi arc, pseudogap, and Lifshitz transitions result from global reconstructions and interferences of poles and zeros with doping to the Mott insulator. The reconstructions are caused by a drastic relaxation of the doublon-holon binding at tiny doping. The criticality at $\delta \to 0$ and a mechanism of the relaxation, though we have given a qualitative picture, should further be clarified in the future. It is also desired to confirm our results in larger-cluster calculations.

We thank Y. Z. Zhang for useful comments. S. S. also thanks S. Watanabe, Y. Yanase, G. Sangiovanni, and D. Tahara for valuable discussions. This work is supported by a Grant-in-Aid (No. 18043008) from MEXT, Japan.

[1] M. R. Norman *et al.*, Nature (London) **392**, 157 (1998).
[2] J. Chang *et al.*, New J. Phys. **10**, 103016 (2008).
[3] N. Doiron-Leyraud *et al.*, Nature (London) **447**, 565 (2007); E. A. Yelland *et al.*, Phys. Rev. Lett. **100**, 047003 (2008); A. F. Bangura *et al.*, *ibid.* **100**, 047004 (2008).
[4] Y. Yanase *et al.*, Phys. Rep. **387**, 1 (2003); R. Preuss, W. Hanke, and W. von der Linden, Phys. Rev. Lett. **75**, 1344 (1995); R. Preuss *et al.*, *ibid.* **79**, 1122 (1997).
[5] B. Kyung *et al.*, Phys. Rev. B **73**, 165114 (2006); Y. Z. Zhang and M. Imada, *ibid.* **76**, 045108 (2007).
[6] E. Dagotto, F. Ortolani, and D. Scalapino, Phys. Rev. B **46**, 3183 (1992); P. W. Leung *et al.*, *ibid.* **46**, 11 779 (1992); Y. Ohta *et al.*, *ibid.* **46**, 14 022 (1992).
[7] D. Sénéchal and A.-M. S. Tremblay, Phys. Rev. Lett. **92**, 126401 (2004).
[8] A. Macridin *et al.*, Phys. Rev. Lett. **97**, 036401 (2006); E. Gull *et al.*, Europhys. Lett. **84**, 37 009 (2008).
[9] M. Civelli *et al.*, Phys. Rev. Lett. **95**, 106402 (2005).
[10] T. D. Stanescu and G. Kotliar, Phys. Rev. B **74**, 125110 (2006); T. D. Stanescu *et al.*, Ann. Phys. (N.Y.) **321**, 1682 (2006).
[11] K. Haule and G. Kotliar, Phys. Rev. B **76**, 104509 (2007).
[12] M. Civelli, arXiv:0808.3948.
[13] A. Avella and F. Mancini, Phys. Rev. B **75**, 134518 (2007).
[14] R. M. Konik, T. M. Rice, and A. M. Tsvelik, Phys. Rev. Lett. **96**, 086407 (2006); K.-Y. Yang, T. M. Rice, and F.-C. Zhang, Phys. Rev. B **73**, 174501 (2006).
[15] M. Aichhorn *et al.*, Phys. Rev. B **74**, 024508 (2006).
[16] I. M. Lifshitz, Zh. Eksp. Teor. Fiz. **38**, 1569 (1960) [Sov. Phys. JETP **11**, 1130 (1960)]; Y. Yamaji, T. Misawa, and M. Imada, J. Phys. Soc. Jpn. **75**, 094719 (2006).
[17] T. A. Maier, T. Pruschke, and M. Jarrell, Phys. Rev. B **66**, 075102 (2002); Y. Kakehashi and P. Fulde, Phys. Rev. Lett. **94**, 156401 (2005).
[18] K. Hanasaki and M. Imada, J. Phys. Soc. Jpn. **75**, 084702 (2006).
[19] I. Dzyaloshinskii, Phys. Rev. B **68**, 085113 (2003).
[20] G. Kotliar *et al.*, Phys. Rev. Lett. **87**, 186401 (2001).
[21] E. R. Gagliano and C. A. Balseiro, Phys. Rev. Lett. **59**, 2999 (1987).
[22] We have confirmed by the CDMFT + quantum Monte Carlo method for a 4×4 cluster at a low temperature $T = 0.1t$ that the cumulants between sites beyond the 2×2 cluster are substantially small. This supports the validity of our results for the 2×2 cluster.
[23] The electronic structure is symmetric around $\omega = 1.46t$ at $\delta = 0$ due to the particle-hole symmetry.
[24] T. Misawa and M. Imada, Phys. Rev. B **75**, 115121 (2007); T. Misawa, Y. Yamaji, and M. Imada, J. Phys. Soc. Jpn. **75**, 083705 (2006); M. Imada, Phys. Rev. B **72**, 075113 (2005).
[25] J. M. Luttinger, Phys. Rev. **119**, 1153 (1960).
[26] $\mathrm{Im}\Sigma$ might also acquire a finite width in the thermodynamic limit while the present finite-cluster calculation cannot reproduce it. When $\mathrm{Im}\Sigma$ is broadened, the zero surface of G is defined by the peak positions of $\mathrm{Im}\Sigma$.